Dalton Transactions

ROYAL SOCIETY OF CHEMISTRY

PAPER

View Article Online
View Journal | View Issue

Cite this: *Dalton Trans.*, 2025, **54**, 3287

Identification of novel triazolylquinoxaline-based metal complexes supported by experimental and virtual screenings†

Laura Holzhauer, [a] Vitalii Shekhovtsev,[b] Cecilia Bruschi,[c] Mathis Gunther,[a] Olaf Fuhr, [b,d] Patrick Hodapp,[e] Claudia Bizzarri, [c] Wolfgang Wenzel, [b] Nicole Jung *[a,d] and Stefan Bräse*[a,c]

The formation of novel complexes from so far non-investigated ligands and different metal centers is important for the development of new functional materials such as (photo)catalysts or biologically active compounds. Still, promising strategies to quickly and systematically investigate the complexation behavior of selected ligands are rare. We developed an NMR-based screening approach to monitor changes within reaction mixtures containing metals and ligands on a small scale *via* a simple but reliable protocol. Based on the obtained data, we could draw conclusions on the formation of 2-(1′,2′,3′-triazol-1′yl)quinoxaline-based transition metal complexes. The NMR screening results obtained were confirmed by the repetition of selected experiments on a large scale, and wherever possible, the type of complex obtained was evaluated by crystal structure elucidation. We could show the versatile complexation of the selected ligands with copper, gold, and silver in a bridging, chelating, or monodentate manner. The calculated theoretical properties supported the experimental results and enabled initial *in silico* predictions of similar compounds before conducting the complexation experiments and structural analyses.

Received 17th July 2024,
Accepted 9th December 2024

DOI: 10.1039/d4dt02068e

rsc.li/dalton

Introduction

The synthesis of novel complexes from different metal centers with so far non-investigated ligands is a promising option to develop new functional materials such as (photo)catalysts,[1] materials for organic light-emitting diodes,[2] and biomedical probes.[3] It may also support the search for new bioactive compounds such as antimicrobial agents.[4] Still, promising strategies for predicting and rapidly detecting complexation processes are rare, and the systematic access to new complexes is difficult. Developing new complexes often relies on coincidental observation or crystallization experiments performed in batch mode. If enough material is available, turbidity measurements can be used for a quantitative observation of the crystallization behavior, although the required equipment and amount of material needed are limiting factors for an establishment as a standard routine.[5] Reported screening methods often use HPLC and LC-MS to detect complexation and are therefore limited to soluble and stable complexes.[6] Moreover, these methods usually focus on synthesizing libraries for an already established type of complex,[3] making them interesting for in-depth biological screenings but not the systematic exploration of complexation properties of new ligands. Due to the lack of techniques for the easy screening of ligands for their potential to form complexes, many combinations of known ligands and metals are probably unknown, and their benefits have not been explored yet. Considering the techniques available in standard organic chemistry labs, we were searching for solutions for the current limitation of fast access to new complexes. NMR-based methods were identified as a simple and fast screening option, being accessible to all synthetic chemists and therefore bearing the potential to systematically investigate the complexation behavior of unknown metal–ligand pairs. Experiments focusing on the investigation of a complexation behavior of metal salts and ligands are established in several academic labs, nevertheless, a systematic

[a]*Institute of Biological and Chemical Systems (IBCS-FMS), Karlsruhe Institute of Technology, Kaiserstraße 12, 76131 Karlsruhe, Germany.*
E-mail: nicole.jung@kit.edu, braese@kit.edu
[b]*Institute of Nanotechnology (INT), Karlsruhe Institute of Technology, Kaiserstraße 12, 76131 Karlsruhe, Germany*
[c]*Institute of Organic Chemistry (IOC), Karlsruhe Institute of Technology, Kaiserstraße 12, 76131 Karlsruhe, Germany*
[d]*Karlsruhe Nano Micro Facility (KNMFi), Karlsruhe Institute of Technology, Kaiserstraße 12, 76131 Karlsruhe, Germany*
[e]*Institute for Biological Interfaces 3 – Soft Matter Synthesis Laboratory (IBG3-SML), Karlsruhe Institute of Technology, Kaiserstraße 12, 76131 Karlsruhe, Germany*

†Electronic supplementary information (ESI) available. CCDC 2336030–2336038. For ESI and crystallographic data in CIF or other electronic format see DOI: https://doi.org/10.1039/d4dt02068e

approach including options for the parallelization of analytical experiments following a defined workflow was not yet described in a similar manner to the best of our knowledge.

Results

In this work, we investigated the potential of standard ^{1}H NMR spectroscopy to screen different ligands and metals for their ability to form novel and so far unknown complexes. In addition, a theoretical approach was tested to evaluate the potential of DFT calculations to support the experimental screening. As a model system, we selected the complexation behavior of triazolylquinoxalines with different metals.

Metal complexes incorporating N-heterocyclic compounds with 1,2,3 triazoles are known as catalysts,[7,8] photosensitizers,[9] and can be applied as live cell imaging probes[10] and for tumor diagnosis[11] amongst other applications.[12,13] Thus, we aimed to gain further insights into the coordination chemistry of triazolylquinoxalines to facilitate the access to novel complexes and to possible new applications of so far unknown metal complexes. Two isomers of triazole-linked N-heterocycles can be distinguished; either the nitrogen or the carbon atoms of the triazole are bound to the quinoxaline. The less common nitrogen-bound form undergoes chelating complexation *via* the nitrogen in position 2 instead of position 1 or 3 as for the carbon-bound form. Therefore, metal complexes with these ligands show differences in their catalytical and photochemical activity, as well as their luminescence intensity, Stokes shift, and lifetime compared to their carbon-bound counterparts.[7,14,15] Some of the rare examples of metal complexes with triazole-linked N-heterocycles bound *via* the nitrogen atom are triazolylquinoxaline-based rhenium complexes. These complexes have been previously described by Bertrand *et al.*[15] and have further been explored by our group, employing pyrazine-substituted triazolylquinoxalines and triazolylimidazo-quinoxalines as ligands.[16] The respective stable rhenium complexes are obtained by reaction of $Re(CO)_5Br$ with the desired ligand in toluene at 110 °C.

Encouraged by these results, we selected the triazolylquinoxaline-based ligands **5a–e** to screen their complexation properties with several other metal centers. These compounds can be straightforwardly synthesized and possess a variation in either the substitution of the triazole or the pyrazine ring of the quinoxaline, allowing to investigate the influence of the molecular structure on the complexation properties of triazolylquinoxalines. The ligands were accessed *via* copper-catalyzed azide–alkyne cycloaddition (CuAAC) from the readily available tetrazolo[1,5-*a*]quinoxaline **2** as previously described in the literature (see Scheme 1).[16,17]

It was intended to investigate the complexation of the selected ligands with different metals by NMR spectroscopy, as this technique is commonly used and readily available in most chemical institutes. ^{1}H NMR measurements present a rapid methodology to observe complexation due to the expected changes of the shifts assigned to the ligand when coordinating

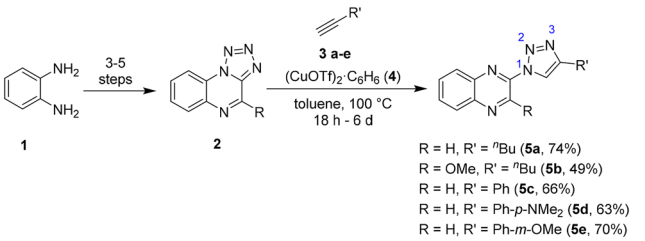

Scheme 1 Synthesis of triazole-bearing ligands **5a–e** for the complexation with different metal centers.[15,16] The numbering of the triazole atom is indicated in blue.

to a diamagnetic metal. For soluble complexes, down- or upfield shifting of selected signals – especially of hydrogen atoms close to the coordinating nitrogen center – is expected. In those cases where the obtained metal complex is less soluble, NMR measurements should reveal a strong depletion up to the complete disappearance of the signals of the ligands. Therefore, an NMR screening combines beneficial aspects for monitoring the complexation of insoluble and soluble complexes. The process allows the indirect detection of insoluble complexes and monitors the progress of the complexation where missing.

To exploit the potential of an NMR-based screening method for a systematic investigation of the coordination potential of different ligands to different metals, processes for homo- and heteroleptic complexes were defined. For a homoleptic screening with 12 different metal salts **6–17** (Table 1), stock solutions of the ligands **5a–c** and an appropriate amount of metal salt were added to an NMR tube. Deuterated methanol was selected as a solvent due to its suitability for comparable experiments with benzotriazole as a ligand.[18] The tubes were then shaken for 30 minutes to ensure thorough mixing of the metal precursor and the ligand for the reaction. Subsequently, NMR spectra of these samples were recorded. Successful complexation led to either a shift of the signal or a decrease of the ligand signals and their disappearance, indicating full conversion to one or more insoluble complexes. $AgNO_3$, $AgSO_3CF_3$, $AgCO_2CF_3$, and $RuCl_3$ promptly complexed with all three ligands, causing a shift for the aromatic signals and, most conspicuously, for the triazole hydrogen atom (8.7 ppm for ligand **5a**, see Fig. 1). For $AuBr_3$, the ligand signals disappeared almost completely due to the precipitation of the obtained complex. The NMR spectra of the successful experiments with ligand **5a** are depicted in Fig. 2; the spectra for ligands **5b** and **5c** as well as for the remaining metals are given in the ESI (Fig. S2–S9†).

When no complexation could be observed in the first measurement at ambient temperature, the samples were subjected to a follow-up experiment. The samples were transferred to a suitable reaction vial, heated to 65 °C for 4 h, and the ^{1}H NMR measurements were repeated. After heating, a complexation with precipitation was observed for the samples with $PdCl_2$ (see Fig. 2), but no change in ^{1}H NMR was observed for the remaining metal centers. In the latter cases, the complexa-

Table 1 Summary of the screening results of ligands **5a–5c** with the 12 different metal precursors **6–17**. The complexation behavior was evaluated by comparing the ^{1}H NMR spectra of free ligands with the reaction mixture, including the metal precursor. ✓ = formation of a complex, ✓* = formation of a complex after heating, x = no complexation observed, x* = decomposition of ligand after heating

Metal ligand	$AgNO_3$ (**6**)	Ag_2CO_3 (**7**)	$AgSO_3CF_3$ (**8**)	$AgOCOCH_3$ (**9**)	$AgOCOCF_3$ (**10**)	$AuBr_3$ (**11**)	$PdCl_2$ (**12**)	$RuCl_3$ (**13**)	$IrCl_3$ (**14**)	$EuCl_3$ (**15**)	$La(NO_3)_3$ (**16**)	$ZnCl_2$ (**17**)
5a	✓	x	✓	x	✓	✓	✓*	✓	x	x	x	x
5b	✓	x	✓	x*	✓	✓	✓*	✓	x*	x	x	x
5c	✓	x	✓	x	✓	✓	✓*	✓*	x	x	x	x

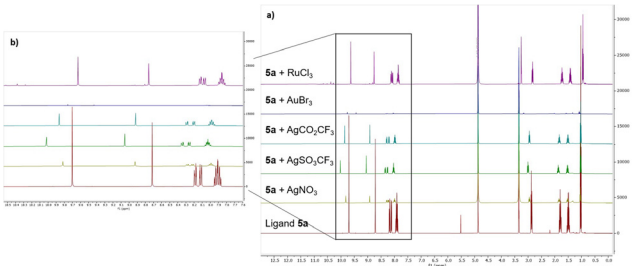

Fig. 1 (a) ^{1}H NMR spectra of ligand **5a** in MeOD before and after the addition of selected metal precursors (ligand concentration: 15 mg mL^{-1}, 1 equiv. of metal precursor). The shifted aromatic signals indicate a successful ligand complexation with these metal centers. (b) Zoom into the region from 7.50 to 10.50 ppm, highlighting changes in the aromatic area of the ^{1}H NMR spectra.

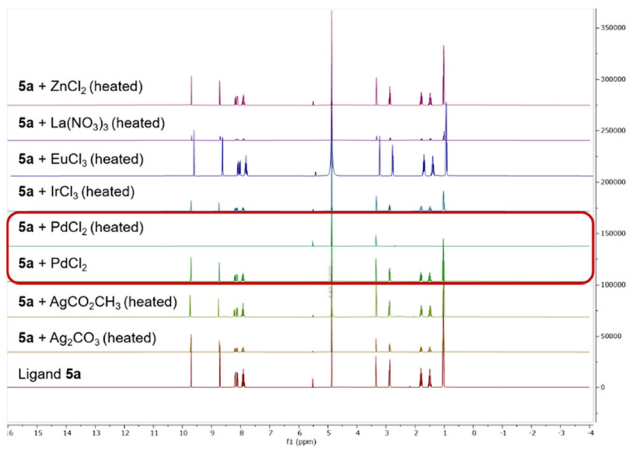

Fig. 2 ^{1}H NMR measurements of ligand **5a** in MeOD without and with different metal precursors after heating to 65 °C for 4 h. For $PdCl_2$, the ligand signal disappeared after the heating step, indicating a complexation-induced precipitation. No complexation process was confirmed with the obtained data for the other metal precursors.

tion was assumed to be unsuccessful. The shifts in the NMR spectra between different ligands and complexes with the same metal precursors are similar in all cases, leading to the assumption that the same coordination mode is present in all investigated complexes with the same metal precursor.

After the NMR-based screening experiments, the complexation with selected metals was repeated in batch synthesis to confirm the formation of the complexes and the expected type of coordination. Ligand **5a** was employed for these experiments and was combined with all metal centers that showed successful complexation, according to Table 1. Using $AgNO_3$ (**6**) as a precursor, a colorless solid precipitated and could be filtered from the reaction mixture to yield complex **18a** in 72% yield. Similar to the NMR experiment, the bulk of the complex precipitated but was still soluble enough to be detected by ^{1}HNMR. We were not able to crystallize the formed complex **18a** from MeOH or MeOD. Suitable crystals were grown from a solution in DMSO-d_6 allowing the elucidation of the product structure **18b** *via* single-crystal X-ray crystallography. The obtained metallacycle consists of two triazolylquinoxaline ligands, two silver atoms, and four nitrate ligands (see Scheme 2). The N3-atom of the triazole and the pyrazine nitrogen each coordinate to a silver atom, linking the dimer in an almost planar configuration. The coordination of the triazole through the N3 donor to the Ag(I) is consistent with related literature-known complexes.[19] The complex crystallizes in the monoclinic space group *P*21/*n* with N–Ag bond lengths of 2.309 and 2.310 Å, only slightly longer than for reported dimeric benzotriazole analogues.[18] A comparison of **18a** and **18b** *via* powder X-ray diffractometry (PXRD) reveals that both complexes are monoclinic but cannot be considered as isostructural.

Using $AgSO_3CF_3$ (**8**) with the same ligand led to the formation of a coordination polymer (**19**) instead of the previously described dimer. A suitable single crystal was obtained

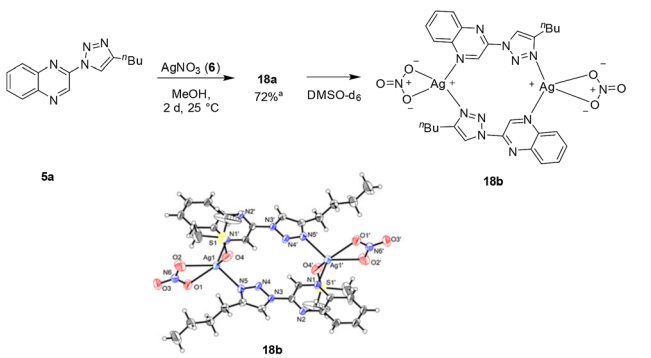

Scheme 2 Reaction of triazolylquinoxaline **5a** with silver nitrate: formation of so far not elucidated compound **18a** and the dimeric [2 + 2] metallacycle **18b** gained from crystallization in DMSO-d_6 including ORTEP diagram of the complex **18b** with the thermal ellipsoids shown at 50% probability. [a]Yield was calculated based on a molecular composition according to **18b** (ratio of $AgNO_3$: 5a = 1 : 1).

from a diluted solution of the obtained precipitate in MeOH. The oxygen atoms of the nitrate counterion are replaced by further complexation to the next quinoxaline unit (see Scheme 3), creating a one-dimensional polymer where the silver atom is coordinated to four nitrogen atoms originating from the pyrazine and the N3-atom of the triazole. The triflate anion is incorporated as a counterion into the structure without direct bonding to the silver atom. The replacement of the counterion might be due to the more electron-deficient nature of the triflate oxygen compared to those in the nitrate counterion, causing the coordination of the quinoxaline to be favored above that of the oxygen. With N–Ag bond lengths of 2.2532 Å to 2.4168 Å, the four bonds are slightly distorted but still in the same range as the related dimeric complex. The chemical shifts of the complexation products of ligand **5a** with $AgNO_3$ and $AgSO_3CF_3$ differ slightly. Similar to the experiments of ligand **5a** with $AgNO_3$ and $AgSO_3CF_3$, the reaction of **5a** with $AgOCOCF_3$ gave a precipitate, indicating the formation of a complex. Nevertheless, no suitable single crystal could be obtained in the batch experiment. A similar coordination mode as for the silver complexes **18b** and **19** is expected; the obtained mass data and the similar chemical shifts in the ^{1}H NMR (see Fig. S10 and Table S1 in the ESI†) support this evaluation.

Complexation attempts with $AuBr_3$ (**11**) and ligand **5a** were carried out in methanol at 25 °C. As already observed in the NMR screening, the complex **20** precipitated quickly as a red solid and could be obtained in 78% by filtration from the reaction mixture. A single crystal suitable for X-ray diffraction was obtained from the slow evaporation of a diluted methanol solution under ambient conditions. The complexation of the square planar Au(III) occurs *via* the N3-atom of the triazole without the involvement of the pyrazine nitrogen atoms, whereas all three bromine atoms remain bound to the gold (Scheme 4). The complex crystallizes in the monoclinic $P2_1/c$ space group with an Au–N distance of 2.040 Å. The observed complexation mode and the distance between the nitrogen and metal center are analogous to the results obtained for a CH_2-spaced complex reported in the literature.[20] For $PdCl_2$ and $RuCl_3$, no suitable single crystals could be grown from the precipitated reaction mixture in the batch experiment. Due to the low solubility of the palladium complex, no conclusion regarding the complexation mode could be drawn from the NMR data. Nevertheless, the obtained mass data indicates the formation of a dimeric complex with two involved triazolylquinoxaline ligands similar to literature-reported benzotriazole palladium complexes[18,21] and other triazole-containing complexes.[22–24] For the ruthenium complex, a trimeric complex with three ligand molecules and one central ruthenium atom is assumed to be present in analogy to the literature.[25,26] The assumed complexation through the triazole nitrogen is supported by the downfield shift of the proton linked to the triazole in the ^{1}H NMR spectrum, similar to the other complexes (see also Fig. S11 and S16 in the ESI†).

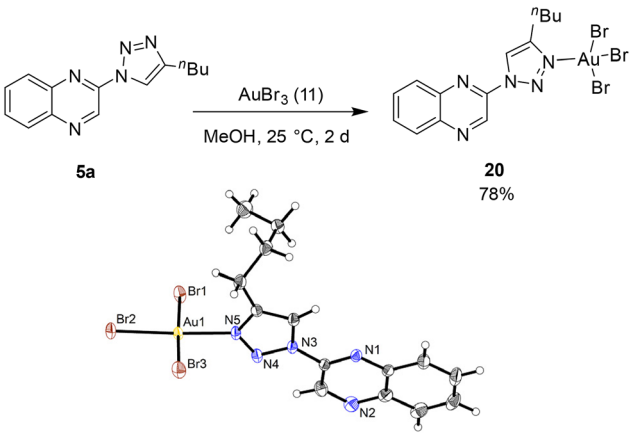

Scheme 4 Synthesis of the monodentate gold(III) triazolylquinoxaline complex **20** and ORTEP diagram of the complex with the thermal ellipsoids shown at 50% probability. ✓ = formation of a complex, x = no complexation observed.

The approach described for homoleptic complexes was expanded to heteroleptic complexes. For the investigation of triazolylquinoxaline-based copper–phosphine complexes, it was decided to additionally include ligands **5d–e** with substituted aromatic residues on the triazole as we deemed those to be the most promising examples for a potential application in photocatalysis in analogy to previously published examples.[9,27] Stock solutions of bis[(2-diphenylphosphino)phenyl] ether (DPEPhos, **23**) or 4,5-bis(diphenylphosphino)-9,9-dimethylxanthene (XantPhos, **24**) were mixed in an NMR tube with

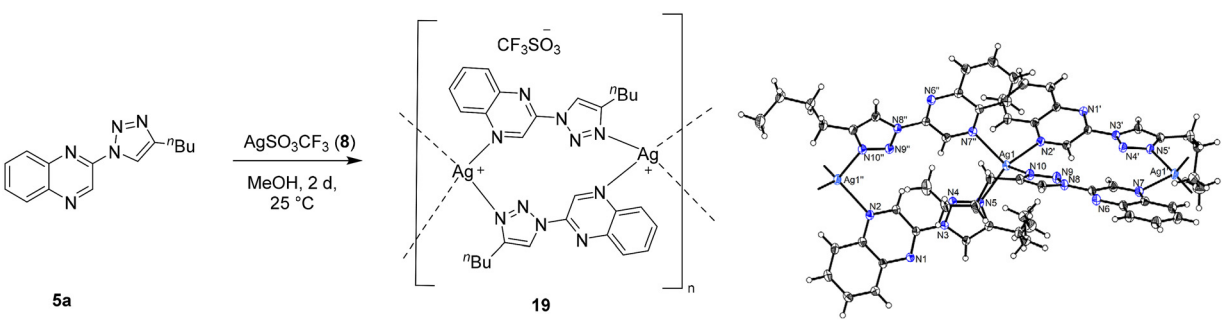

Scheme 3 Synthesis of the polymeric complex **19** and ORTEP diagram of the complex with the thermal ellipsoids shown at 50% probability.

either $[Ag(MeCN)_4]BF_4$ or $[Cu(MeCN)_4]BF_4$ as precursors. Here, DCM-d_2 was employed, following previous reports on heteroleptic Cu(I) and Ag(I) complexes.[27,28] The solutions were shaken for 20–30 min, then a solution of the triazolylquinoxaline ligand was added, and the mixture was shaken for another 20–30 min before the ^{1}H NMR measurement was conducted. A successful complexation of the triazolylquinoxaline ligand was observed for all the combinations (see Table 2 and Fig. 3), in accordance with literature describing similar complexes.[29] Again indicated by the shift of the aromatic signals of the quinoxaline and, most remarkably, the triazole hydrogen atom. The spectra for experiments with ligands **5a** and **5b–e** are respectively given in Fig. 3 and in the ESI section (Fig. S12–S15†).

The heteroleptic triazolylquinoxaline-phosphine silver complex **25** was synthesized in batch and fully analyzed, and the structure could be confirmed *via* single-crystal X-ray diffraction (Scheme 5). A suitable crystal was obtained through vapor diffusion with DCM and diethyl ether. The X-ray analysis highlighted that compound **5a** acted as monodentate ligand, being coordinated only through the N5-nitrogen of the triazole moiety.

Three heteroleptic copper complexes **26a**, **26b**, **26c** were synthesized following a previously published procedure,[30] adding the diimine ligand to a dried dichloromethane solution of the Cu(I) precursor $[Cu(MeCN)_4]BF_4$ and the chelating DPEPhos ligand, under an argon atmosphere. After 4 hours of reaction, the solvent was removed under vacuum, and the three copper complexes were obtained as red powders. Lastly, the three mononuclear complexes formed crystals by slow diffusion of a cyclohexane layer into a concentrated dichloromethane solution, achieving high purity with reaction yields of 77% for **26a**, 84% for **26b** and 76% for **26c** (Scheme 6). The obtained crystals were suitable for single-crystal X-ray crystallography. These copper complexes crystallize in the triclinic system with a $P\bar{1}$ space group. The three compounds show similar distances between the metal center and the central nitrogen atom of the triazole unit (2.063 Å for **26a**, 2.060 Å for **26b**, 2.067 Å for **26c**), while the distance between the copper and the nitrogen atom of the quinoxaline ring is slightly smaller for **26a** (2.061 Å)

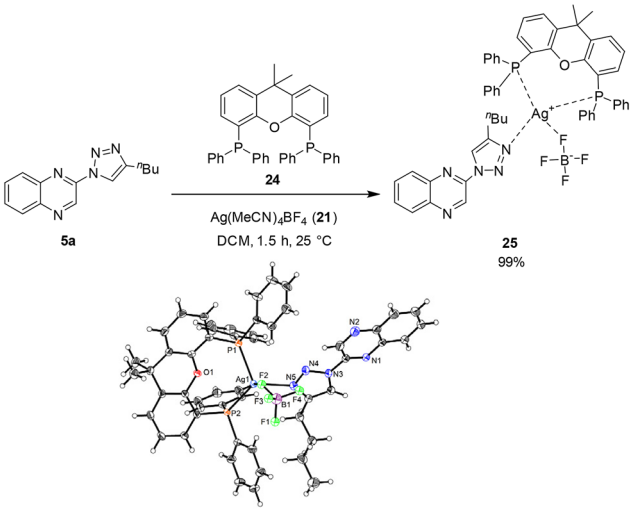

Scheme 5 Synthesis of the heteroleptic phosphine silver complex **25** and ORTEP diagram of the complex with the thermal ellipsoids shown at 50% probability.

Table 2 Screening of ligands **5a–5e** in combination with two different chelating phosphines and Ag(I) or Cu(I) as metal centers. ✓ = formation of a complex, x = no complexation observed

	$[Ag(MeCN)_4]BF_4$ (**21**)		$[Cu(MeCN)_4]BF_4$ (**22**)	
Ligand	DPEPhos (**23**)	XantPhos (**24**)	DPEPhos (**23**)	XantPhos (**24**)
5a	✓	✓	✓	✓
5b	✓	✓	✓	✓
5c	✓	✓	✓	✓
5d	✓	✓	✓	✓
5e	✓	✓	✓	✓

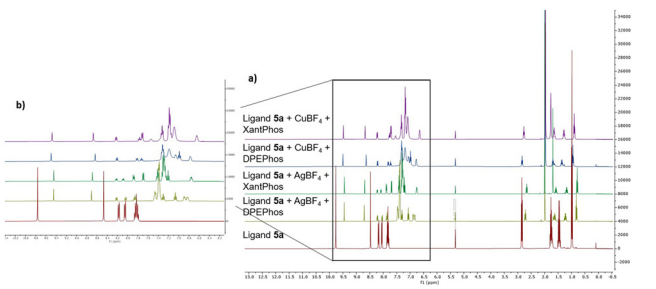

Fig. 3 (a) ^{1}H NMR spectra of ligand **5a** and the corresponding complexes obtained by reaction with $[Ag(MeCN)_4]BF_4$ or $[Cu(MeCN)_4]BF_4$ (abbreviated as $AgBF_4$ and $CuBF_4$ in the figure for conciseness) and the phosphine ligands DPEPhos or XantPhos in DCM-d_2. (b) Zoom into the region from 6.20 to 10.40 ppm, highlighting changes in the aromatic area of the ^{1}H NMR spectra.

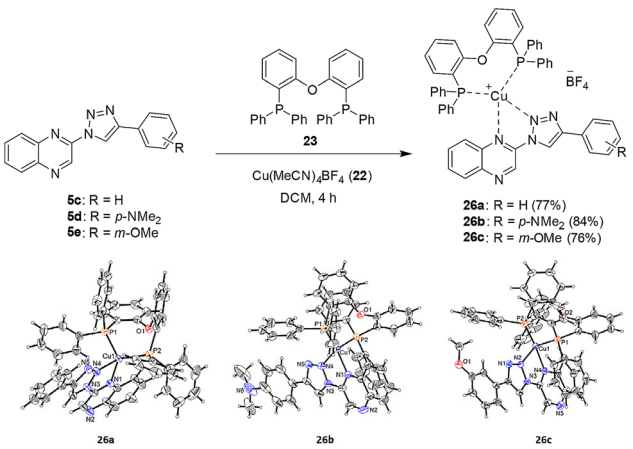

Scheme 6 Synthetic procedure for the mononuclear copper complexes **26a–c** and ORTEP drawing of crystals **26a** (left), **26b** (center), **26c** (right). Counterions and solvent molecules were omitted for clarity.

than the ones of **26b** (2.089 Å) and **26c** (2.084 Å), that are almost identical. The distances between the copper and the coordinative P atoms of the chelating diphosphine are quite similar for all three compounds (**26a**: 2.256 Å, **26b**: 2.220 Å, **26c**: 2.213 Å for Cu–P_1 and **26a**: 2.210 Å, **26b**: 2.275 Å, **26c**: 2.286 Å for Cu–P_2). Lastly, the three complexes show similar bite angles N1–Cu–N4 (**26a**: 78.93°, **26b**: 77.74°, **26c**: 77.6°) and P1–Cu–P2 (**26a**: 115.67°, **26b**: 113.15°, **26c**: 117.44°). These values are typical of a pseudo-tetrahedral geometry and match those of previously published copper complexes with related structures.[9,31] The present chelating coordination mode is in contrast to the monodentate complexation observed for the heteroleptic phosphine silver complexes (see above).

When comparing the ^{1}H NMR spectra of all complexes elucidated above, a complexation-dependent shift of the isolated hydrogen atoms of the pyrazine and triazole is visible, showing the power of NMR screening techniques to distinguish between coordination modes (see Fig. S16, ESI†). Depending on the involvement of the quinoxaline unit in the complex, the pyrazine hydrogen atom is de-shielded or more shielded than the ligand.

In addition to the experimental screenings and batch syntheses, theoretical calculations with density functional theory (DFT) were conducted to analyze the screening results further. The computations were carried out with the hybrid range separated CAM-B3LYP functional[32] combined with the def2-SVP basis set by Ahlrichs and coworkers including relativistic effective core potential for Au and Ag atoms.[33] The energy of ligand **5a** was calculated depending on the rotation around the connecting C–N bond, showing the difference in the stability of the two major conformations labeled as "bridging" and "chelating" (Fig. 4a). In the bridging conformation, the triazole nitrogen atoms face inwards and the rotational energy is minimal. This conformation is not only lower in energy according to the computational data, but also the preferred conformation observed experimentally in the crystal lattice (see Fig. S17, ESI†). The chelating conformation is presumably destabilized by the repulsion of the triazole and quinoxaline hydrogen atoms (see Fig. 4b). It can be assumed that the ligand will usually adopt the bridging conformation in the absence of a metal or in the presence of a mono-coordinated metal center, and will only remain in the less favorable chelating conformation if a stable chelate complex is formed with a suitable metal.

We intended to obtain theoretical information describing the stability and electronic distribution of complexes **18b–20**, **25**, and **26a** compared to the properties of the ligand **5a** alone. Fig. 5 gives an overview of the complex structures and the notation used for the following paragraphs.

In coordination compounds, elucidating the bonding nature by modeling proves to be complicated. Our approach integrates (1) aromaticity of the ligand (NICS), (2) electrostatic (NBO), and (3) π-backdonation from the metal center to the click ligand (normal mode frequency) mechanisms to elucidate the diverse stabilization phenomena observed across various compounds. To evaluate the aromaticity based on the magnetic properties of the compound, the nucleus-independent chemical shifts (NICS)[34] were computed. Herein, a more negative value is connected to higher aromaticity of the respective moiety and thus increased stabilization effects. The lowest overall shifts among the investigated complexes for the triazole, pyrazine, and phenyl moieties are observed for the gold complex **20** (Fig. 6). The same behavior can be noticed when calculating the out-of-plane $NICS_{zz}$ values, a more accurate variant for most applications.[35] This indicates the highest stability for complex **20** among the investigated 1,2,3-triazolylquinoxaline complexes. The NICS values also help to explain why a monodentate complexation of silver tetrafluoroborate with the ligand in bridging conformation is observed for the heteroleptic silver complex **25**. The $NICS_{zz}$ values for a hypothetical chelating complexation are higher than for the observed complexation in the bridging conformation, suggesting a lower stability for the chelating complexation (see Table S5, ESI†). The same trend is present when switching the ligand from **5a** to **5c**; despite the higher steric hindrance of the phenyl residue in the bridging conformation, the monodentate complexation is still assumed to occur in the silver complex.

Both **5a** and **5c** should be aromatic according to the Hückel rule (molecule **5c** has 22 π electrons and **5a** has 14 π electrons,

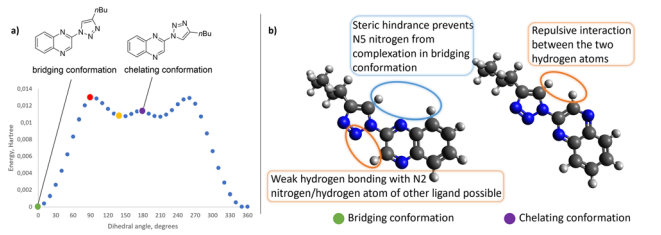

Fig. 4 (a) Energy curve for the rotation of the ligand **5a** around the N–C bond connecting the triazole and quinoxaline. Green dot: bridge conformation, yellow dot: bridge conformation rotated by ~140 degrees about the Sigma bond between the ring moieties, purple dot: chelate conformation (bridge conformation rotated by a straight angle about the Sigma bond between the ring systems), red dot: two ring moieties are at right angle. (b) Structural implications of the most important conformation modes of ligand **5a** for complexation.

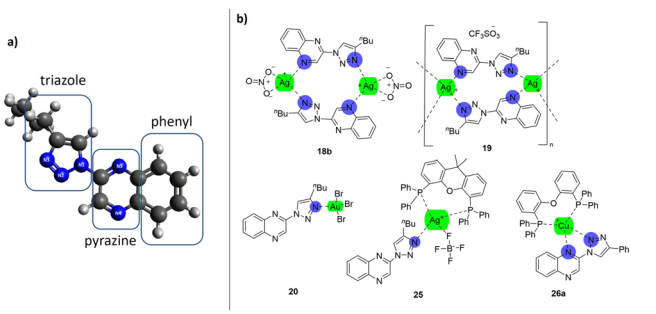

Fig. 5 (a) Moieties for the NICS values and notation for the NBO charges of ligand **5a**. (b) Overview of experimentally confirmed complexation motifs.

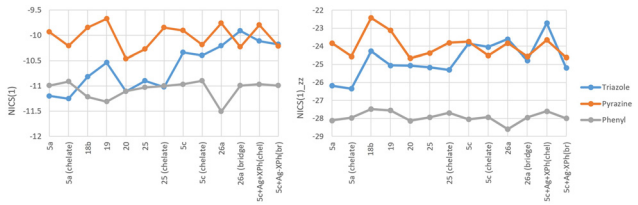

Fig. 6 NICS and out-of-plane $NICS_{zz}$ values for ligands **5a** and **5c** (bridging and chelating conformation) and the complexes **18b–20**, **25** and **26a**. Additionally, computational results for hypothetical chelating complexes in analogy to **25** and **26** and two possible conformations for the complex of ligand **5c** with $AgBF_4$ and XPhos are provided.

both corresponding to $4n + 2$ rule) and according to the NICS, but NICS alone is usually inadequate for assessing aromaticity due to its locality.[36] Visualizing ring currents reveals the aromatic nature of molecules due to delocalized π electrons, aiding in the identification of aromatic systems. Utilizing the CTOCD (continuous transformation of origin of current density) method for gauge selection it is possible to visually inspect the non-local nature of the ring current as well as have structural information.[37] The currents were broken down into currents originating from π manifold and currents from the remaining populated orbitals. When inspecting the molecular current maps (see Fig. S33 and S34, ESI†), it was found that the ring current is diatropic mostly from the π orbitals and consistency with NICS was verified.

The analysis of the natural bond orbitals (NBO) provides explanations for the distribution of atomic charges (see Table S4, ESI†). The N2 and N5 atoms are important for forming the chelate conformation, while the N3 and occasionally N4 atoms are important for the bridging mode. When the chelating conformation is stable, N2 and N5 atoms possess higher charges in this conformation than in the bridge conformation. When the bridging conformation is stable, the N3 and N4 atoms possess higher charges in the bridge conformation than in the chelate conformation. A higher charge on nitrogen atoms near the metal cation accounts for better charge neutralization in different conformations, building up their stabilities. To inspect π-backdonation to the ligand, we compared the frequencies of the normal mode possessing the same symmetry as the LUMO orbital of the ligand **5a** (Fig. S20 in the ESI†) and found that the ligand is not a good π-acceptor as opposed to previous studies,[38] which is reflected in a subtle change in the vibration frequency (Table S4, ESI†).

In addition, exemplary calculations on the complexation energies and Gibbs energies were conducted for complexes **18b–20**, **25**, and **26a**, hypothetical complexes (entries 2, 6, and 7), and entries 9 and 10, without a crystal structure. The obtained energies should give information on the theoretical spontaneity of the respective complex formation step. For this purpose, the reaction of the ligand in the bridging conformation with the respective metal precursor was considered (see ESI for further information, pages 33–38†). The obtained energies support the experimental results; all formed complexes **18b–20**, **25**, and **26** have negative theoretical complexation and Gibbs energies. A complexation of **5a** with silver acetate is not expected due to the positive free Gibbs energy of the reaction (Table 3, entry 2), whereas the exergonic reaction to the other silver complexes **18b**, **19**, and **25**, summarized in Table 3, can occur. The strongly negative free energy of the silver nitrate complexation (**18b**, entry 1) might be related to simplifying the three-dimensional crystal lattice to a separated Ag^+ and NO_3^- pair within the single-molecule modeling approach. A slight tendency toward the bridging conformation of the heteroleptic silver triazolylquinoxaline-phosphine complexation can be derived from entries 5 and 6 as well as 9 and 10. The observed complexation mode seems to be mostly favored due to the higher stability of the final complex (see section above), not only due to the energetically slightly favored formation. For the copper complex **26**, the formation of the experimentally observed chelate complex is predicted to be slightly energetically favored compared to the bridging complexation (entries 7 and 8).

Table 3 Calculated gas-phase complexation energies ΔE and Gibbs energy ΔG of ligands **5a** and **5c** with selected metals. For entries 5 and 6, as well as 9 and 10, XantPhos (**24**) is considered an additional ligand; for entries 7 and 8, DPEPhos (**23**) is considered. For further information on the modeled reaction equations, please refer to the ESI (Fig. S23–S32†)

Entry	Ligand	Metal precursor	Complex	Variant	ΔE [kJ mol^{-1}]	ΔG [kJ mol^{-1}]
1	**5a**	$AgNO_3$	**18b**	—	−1754.89	−1548.31
2	**5a**	$[AgCH_3CO_2]_2$	—	—	−64.5	30.0
3	**5a**	$AgSO_3CF_3$	**19**	—	−1288.74[a]	−921.14[a]
4	**5a**	$AuBr_3$	**20**	—	−124.68	−72.88
5	**5a**	$[Ag(MeCN)_4]BF_4$	**25**	Bridge	−565.37	−483.55
6	**5a**	$[Ag(MeCN)_4]BF_4$	—	Chelate	−556.66	−475.39
7	**5c**	$[Cu(MeCN)_4]BF_4$	—	Bridge	−662.71	−572.98
8	**5c**	$[Cu(MeCN)_4]BF_4$	**26a**	Chelate	−673.50	−579.78
9	**5c**	$[Ag(MeCN)_4]BF_4$	—	Bridge	−557.53	−478.21
10	**5c**	$[Ag(MeCN)_4]BF_4$	—	Chelate	−551.88	−472.12

[a] Polymeric complex structure simplified for calculation as a tetramer with three silver atoms and four additional ammonia atoms to account for the next quinoxaline units.

Conclusions

A screening approach based on NMR spectroscopy for metal complexes with triazolylquinoxaline ligands has been developed to support the systematic investigation of metal complexation for selected examples. The formation of homoleptic complexes with different metals and the triazolylquinoxaline as the lone organic ligand and of heteroleptic complexes with an additional phosphine ligand was successfully investigated using this methodology. Selected complexation reactions were reproduced in batches, and the structures of the obtained complexes were confirmed *via* single-crystal X-ray diffraction, showing the versatility of the employed ligand in monodentate, chelating, and bridging complexes. Additional computations allowed for an increased understanding of the experimentally observed properties and enabled *in-silico* predictions for similar compounds prior to their synthesis. In combination with the observed shifts of characteristic ^{1}H NMR signals, the complexation modes of related compounds can be roughly estimated without crystallographic data. Although the concepts have been only proven to work for a limited number of examples within a very limited chemical space, this work presents a step towards the systematic and accelerated discovery and investigation of metal complexation. The combination of computations and the observed characteristic shifts of the ^{1}H NMR signals depending on the complexation mode can help to predict the complexation behavior for derivatives for which no crystallographic data is available and thus contribute to the accelerated investigation of metal complexation. The shown screening method can be further expanded and customized by using different solvents, additives, and varying equivalents of the metal precursor, thus allowing for a fast, in-depth investigation of the complexation behavior of selected ligands.

Author contributions

LH: methodology, experiments, writing; VS: calculations, writing; CeB: experiments, writing; MG: experiments; OF: crystallography; PH: methodology, 3D design and printing; ClB: supervision; WW: supervision; NJ: conceptualization, supervision; SB: supervision. All authors reviewed and edited the manuscript.

Data availability

The ESI† covers detailed information on the experiments conducted and their results. All experimental details, including the analytical description of the obtained target compounds, are available in the ESI.† Data referring to the experiments described herein were submitted to the repository Chemotion (**https://www.chemotion-repository.net/**). All DOIs minted for the data are linked in the ESI.† New data obtained in this study is assigned to the collection embargo numbers cbu_2022-01-18 (**https://dx.doi.org/10.14272/collection/cbu_2022-01-18**) and LSH_2023-12-07_2 (**https://dx.doi.org/10.14272/collection/LSH_2023-12-07_2**).[39] Further NMR data and the stl.file for the 3D-printed NMR tube mount were deposited in the repository Radar4Chem and are available at **https://dx.doi.org/10.22000/soDUutABNkcCdbHh**. The material obtained in this study was submitted to the Molecule Archive at KIT and can be requested from there (**https://compound-platform.eu/home**). Crystallographic data for compounds **5a**, **5c**, **18b**, **19**, **20**, **25**, **26a**, **26b**, **26c** reported in this paper have been deposited with the Cambridge Crystallographic Data Centre as CCDC 2336030 to 2336038.†

Conflicts of interest

There are no conflicts to declare.

Acknowledgements

L. H. acknowledges funding by the Landesgraduiertenförderung Baden-Württemberg. M. G. acknowledges funding from the ERASMUS program and the Regional International Mobility Scholarship of Lyon. We acknowledge the financial support by the Joint Lab VirtMat (projects P10, P11, P14) within the Helmholtz research area Information and the support by the State of Baden-Württemberg through bwHPC and the German Research Foundation (DFG) through grant no INST 40/575-1 FUGG (JUSTUS 2 cluster) under project bw20F004. We thank Chloé Liagre for synthetic assistance and Prof. Dr Sonja Herres-Pawlis (RWTH Aachen) for discussions and suggestions. We also thank Dr Patrick Weis (KIT-IPC) for additional mass spectrometry measurements conducted in the scope of this project and Peter Weidler (KIT-IFG) for supporting with PXRD measurements for **18a** and **18b**. This work was supported by the Helmholtz program information. We acknowledge support by Deutsche Forschungsgemeinschaft for the DFG-core facility Molecule Archive, to which all target compounds were registered for further re-use (DFG project number: 284178167) and the support of NFDI4Chem (441958208) for the provision and adaptation of the research infrastructure Chemotion repository used in this project. We acknowledge the support of the Open Access Publishing Fund of Karlsruhe Institute of Technology.

References

1 C. Bizzarri, *Eur. J. Org. Chem.*, 2022, e202200185.
2 C. Bizzarri, E. Spuling, D. M. Knoll, D. Volz and S. Bräse, *Coord. Chem. Rev.*, 2018, **373**, 49.
3 M. J. Chow, C. Licona, D. Yuan Qiang Wong, G. Pastorin, C. Gaiddon and W. H. Ang, *J. Med. Chem.*, 2014, **57**, 6043.
4 A. Frei, J. Zuegg, A. G. Elliott, M. Baker, S. Braese, C. Brown, F. Chen, C. G. Dowson, G. Dujardin, N. Jung, A. P. King, A. M. Mansour, M. Massi, J. Moat, H. A. Mohamed, A. K. Renfrew, P. J. Rutledge, P. J. Sadler,

M. H. Todd, C. E. Willans, J. J. Wilson, M. A. Cooper and M. A. T. Blaskovich, *Chem. Sci.*, 2020, **11**, 2627.
5 P. P. Nievergelt and B. Spingler, *CrystEngComm*, 2017, **19**, 142.
6 (*a*) C. C. Konkankit, B. A. Vaughn, S. N. MacMillan, E. Boros and J. J. Wilson, *Inorg. Chem.*, 2019, **58**, 3895; (*b*) S. P. Mulcahy, K. Gründler, C. Frias, L. Wagner, A. Prokop and E. Meggers, *Dalton Trans.*, 2010, **39**, 8177.
7 S. Jindabot, K. Teerachanan, P. Thongkam, S. Kiatisevi, T. Khamnaen, P. Phiriyawirut, S. Charoenchaidet, T. Sooksimuang, P. Kongsaeree and P. Sangtrirutnugul, *J. Organomet. Chem.*, 2014, **750**, 35.
8 (*a*) Y. Yang, W. Hu, X. Ye, D. Wang and X. Shi, *Adv. Synth. Catal.*, 2016, **358**, 2583; (*b*) D. Wang, Y. Yang, R. Huang, L. Wang and H. Wan, *J. Chem. Res.*, 2016, **40**, 645.
9 L.-L. Gracia, L. Luci, C. Bruschi, L. Sambri, P. Weis, O. Fuhr and C. Bizzarri, *Chem. – Eur. J.*, 2020, **26**, 9929.
10 T. U. Connell, J. L. James, A. R. White and P. S. Donnelly, *Chem. – Eur. J.*, 2015, **21**, 14146.
11 N. Roy, U. Sen, Y. Madaan, V. Muthukumar, S. Varddhan, S. K. Sahoo, D. Panda, B. Bose and P. Paira, *Inorg. Chem.*, 2020, **59**, 17689.
12 B. Chowdhury, S. Khatua, R. Dutta, S. Chakraborty and P. Ghosh, *Inorg. Chem.*, 2014, **53**, 8061.
13 (*a*) D. Preston, J. J. Sutton, K. C. Gordon and J. D. Crowley, *Angew. Chem., Int. Ed.*, 2018, **57**, 8659; (*b*) J. D. Crowley and P. H. Bandeen, *Dalton Trans.*, 2010, 612.
14 W. K. C. Lo, G. S. Huff, J. R. Cubanski, A. D. W. Kennedy, C. J. McAdam, D. A. McMorran, K. C. Gordon and J. D. Crowley, *Inorg. Chem.*, 2015, **54**, 1572.
15 H. C. Bertrand, S. Clède, R. Guillot, F. Lambert and C. Policar, *Inorg. Chem.*, 2014, **53**, 6204.
16 L. Holzhauer, C. Liagre, O. Fuhr, N. Jung and S. Bräse, *Beilstein J. Org. Chem.*, 2022, **18**, 1088.
17 B. Chattopadhyay, C. I. R. Vera, S. Chuprakov and V. Gevorgyan, *Org. Lett.*, 2010, **12**, 2166.
18 C. Richardson and P. J. Steel, *Dalton Trans.*, 2003, 992.
19 M. L. Gover and J. D. Crowley, *Dalton Trans.*, 2010, **39**, 2371.
20 M. Bortoluzzi, A. Scrivanti, A. Reolon, E. Amadio and V. Bertolasi, *Inorg. Chem. Commun.*, 2013, **33**, 82.
21 S. A. Al-Jibori, L. A. Al-Doori, A. S. Al-Janabi, M. A. Alheety, H. Akbaş and A. Karadag, *J. Mol. Struct.*, 2020, **1207**, 127832.
22 M. Xia, Y. Chen, Z. Chen, W. Yu, H. Cheng, C. Feng and P. Hu, *Liq. Cryst.*, 2022, **49**, 72.
23 P. S. Gahlaut, D. Gautam, P. Lama and B. Jana, *New J. Chem.*, 2023, **47**, 6871.
24 J. D. Crowley and E. L. Gavey, *Dalton Trans.*, 2010, **39**, 4035.
25 (*a*) L. Todorov and I. Kostova, *Front. Chem.*, 2023, **11**, 1247805; (*b*) P. I. P. Elliott, in *Organometallic Chemistry*, ed. I. J. S. Fairlamb and J. M. Lynam, Royal Society of Chemistry, Cambridge, 2014, vol. 39, pp. 1–25.
26 J. T. Fletcher, B. J. Bumgarner, N. D. Engels and D. A. Skoglund, *Organometallics*, 2008, **27**, 5430.
27 C. Bruschi, X. Gui, N. Salaeh-arae, T. Barchi, O. Fuhr, S. Lebedkin, W. Klopper and C. Bizzarri, *Eur. J. Inorg. Chem.*, 2021, **2021**, 4074.
28 J.-H. Jia, D. Liang, R. Yu, X.-L. Chen, L. Meng, J.-F. Chang, J.-Z. Liao, M. Yang, X.-N. Li and C.-Z. Lu, *Chem. Mater.*, 2020, **32**, 620.
29 C. Bruschi, X. Gui, P. Rauthe, O. Fuhr, A. N. Unterreiner, W. Klopper and C. Bizzarri, *Chem. – Eur. J.*, 2024, **30**, e202400765.
30 C. Bizzarri, C. Strabler, J. Prock, B. Trettenbrein, M. Ruggenthaler, C.-H. Yang, F. Polo, A. Iordache, P. Brüggeller and L. de Cola, *Inorg. Chem.*, 2014, **53**, 10944.
31 C. Bizzarri, A. P. Arndt, S. Kohaut, K. Fink and M. Nieger, *J. Organomet. Chem.*, 2018, **871**, 140.
32 T. Yanai, D. P. Tew and N. C. Handy, *Chem. Phys. Lett.*, 2004, **393**, 51.
33 F. Weigend and R. Ahlrichs, *Phys. Chem. Chem. Phys.*, 2005, **7**, 3297.
34 Z. Chen, C. S. Wannere, C. Corminboeuf, R. Puchta and P. V. R. Schleyer, *Chem. Rev.*, 2005, **105**, 3842.
35 F. Alvarez-Ramírez and Y. Ruiz-Morales, *J. Chem. Inf. Model.*, 2020, **60**, 611.
36 P. Lazzeretti, *Phys. Chem. Chem. Phys.*, 2004, **6**, 217.
37 T. A. Keith and R. F. Bader, *Chem. Phys. Lett.*, 1993, **210**, 223.
38 D. Urankar, B. Pinter, A. Pevec, F. de Proft, I. Turel and J. Kosmrlj, *Inorg. Chem.*, 2010, **49**, 4820.
39 L. Holzhauer, C. Bruschi, M. Gunther and C. Liagre. Chemotion Repository, 2024; **https://dx.doi.org/10.14272/collection/LSH_2023-12-07_2** and **https://dx.doi.org/10.14272/collection/cbu_2022-01-18**.